Diagnostic Comparisons of Near-Earth Object Identification using Slit Spectroscopy and Slitless Grating Methods

Eileen V. Ryan and William H. Ryan
Magdalena Ridge Observatory, New Mexico Institute of Mining and Technology
101 East Road, Socorro, NM 87801

ABSTRACT

Space object identification and characterization is an important component of Space Situational Awareness (SSA). However, characterization of natural objects such as asteroids that pass close to the Earth is also a useful endeavor both scientifically, and for reasons related to hazard mitigation of potential Earth-impacting bodies. Therefore, researchers at the Magdalena Ridge Observatory (MRO) 2.4-meter telescope (located in New Mexico) have been investigating the option to utilize SSA-inspired techniques and equipment to characterize both classes of these target-of-opportunity objects. The goal is to develop a methodology that returns useful diagnostic information with a minimal investment in observational preparation since typically there can be little warning when interesting asteroids or satellites are in prime viewing geometry. Merging these objectives into our operational paradigm to capitalize on the dual-use nature of the instrumentation ensures that the MRO facility is ready to meet any prospective opportunity.

A collaboration between the Air Force and MRO to enhance SSA techniques has provided both a visible wavelength, low-resolution spectrometer, and a filter-wheel mounted grating system (Dao, et al. 2013) used on the 2.4-meter telescope. In 2012, efforts began to extend this instrumentation beyond its SSA applications to the study of near-Earth asteroids (NEAs). Although the slit-based spectrometer has proven very successful in identifying target material type and is set up for rapid deployment, it is not configured for instantaneous access and requires some preparation time. The purpose of this current effort is to examine whether a filter-wheel mounted grating with immediate availability might be sufficient to acquire spectra with a quality level adequate for rough taxonomic classification of (almost) no warning, target of opportunity near-Earth asteroids.

1. INTRODUCTION

The typical lifetimes of NEAs are up to three orders of magnitude shorter than the typical timescales associated with the main asteroid belt. Therefore, the current NEA population is a relatively recent product that has to be continually re-supplied. Spectroscopic analysis of NEAs helps characterize their taxonomic distribution and identify potential source regions which would then enhance our understanding of the origin of the current population. Although this is of interest scientifically, it can also help estimate the magnitude of the hazard threat from still undiscovered asteroids as well as provide guidance to optimize ground-based telescope search strategies.

NEA discovery surveys have been extremely prolific in the last decades and have made considerable progress toward the goal of cataloging Near Earth Asteroids (NEAs) larger than about 100 meters in diameter. Moreover, astrometric follow-up efforts (by the NASA surveys and follow-up facilities and the citizen-scientist astronomy community) have resulted in reliable orbit determinations for thousands of NEAs. However, there still remains many uncertainties regarding the nature of the NEA population, and hence, the development of mechanisms for assessing and alleviating any associated hazards suffer as a result. With the advent of planned human spaceflight missions to explore NEAs, a better understanding of the populations' physical properties is essential to guide target selection (picking an object of an appropriate size, with a feasible spin rate, and a desirable composition) and strategic investigation of potential deflection mechanisms. Better assessment of hazard based on object size is also valuable.

Most NEA diameters are determined indirectly from their albedos. However, less than 1% of the NEAs have albedo measurements and an assumed value of ~0.15 is usually used. Therefore, since the measured values range from 0.02 to 0.63 (Binzel et al. 2002), this assumption can lead to diameter uncertainties of a factor of ~2. In the absence of better albedo determinations, which require simultaneous visible and thermal IR observations, it is possible to minimize this diameter uncertainty by identifying an object's taxonomic classification through more easily obtainable visible and/or near-IR spectra. Figure 2 illustrates the usefulness of this spectral range for rough taxonomic grouping. Since the albedo scatter within taxonomic classes is significantly less, this is a desirable constraint. Despite the name, the Small Main-belt Asteroid Spectroscopic Survey (SMASS) has been routinely acquiring NEA spectra since the early 1990's (Binzel et al. 2004). Stuart and Binzel (2004) re-evaluated the NEA size distribution and impact hazard based on these compositional results. We use the SMASS database as a reference library to classify the spectra we obtain as part of our program which uses a low-resolution visible spectrometer.

Figure 1 illustrates the usefulness of this spectral range for rough taxonomic grouping. Since the albedo scatter within taxonomic classes is significantly less, this is a desirable constraint. Despite the name, the *Small Main-belt Asteroid Spectroscopic Survey* (SMASS) has been routinely acquiring NEA spectra since the early 1990's (Binzel et al. 2004). Stuart and Binzel (2004) re-evaluated the NEA size distribution and impact hazard based on these compositional results. We use the SMASS database as a reference library to classify the spectra we obtain as part of our program to determine asteroid material type.

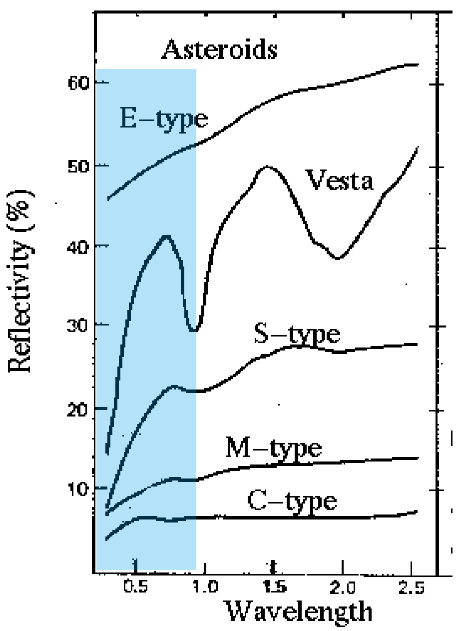

Fig. 1. Highlighted in blue is the wavelength range covered by the Magdalena Optical Spectroscopy System (MOSS), about 0.3 – 0.9 microns. Sample spectra for different asteroid taxonomic classes are shown. Even though this small range is not fully diagnostic (pairing it with IR spectra would be ideal), it is adequate to make first-order taxonomic identifications that lead to better constraints on albedo and thereby NEA size.

In the following section we describe two approaches to obtaining asteroid spectra: slit-based spectroscopy and slitless grating spectroscopy. The goal is to determine whether a lower resolution (by a factor of 10 with respect to the slit-based spectrometer), readily available slitless grating is sufficient for rough taxonomic classification in the study of target-of-opportunity NEAs.

2. SPECTROSCOPY OF NEAR-EARTH ASTEROIDS

Asteroid spectra are typically obtained at MRO using the Magdalena Optical Spectroscopy System (MOSS), a slit based spectrometer that was initially developed for the purpose of artificial targets (e.g., satellites). Although the MOSS instrument has proven very successful in identifying asteroid material type and is set up for rapid deployment, it is it is not configured for instantaneous access and requires *some* preparation time. The purpose of this current effort is to examine whether a filter-wheel mounted grating with *immediate* availability might be sufficient to acquire spectra with a quality level adequate for rough taxonomic classification of (almost) no warning, target of opportunity near-Earth asteroids.

Prototype Slitless Grating Configuration

A prototype of this open grating system was already developed for observations of artificial targets. The grating system on the 2.4-meter telescope consists of a blazed 100 line/mm transmission grating mounted in the facility filter wheel for easy accessibility. This places the grating in an f/8.9 converging beam approximately 195 mm in front of the focal plane. The resulting first order spectra have a dispersion of 56.2 nm/mm with a length of ~9 mm over the wavelength range 400 to 900 nm. The spectra are imaged using an Andor iKon 936 CCD camera with a *2Kx2K* EEV CCD42-40 array and 13.5 micron pixels thermoelectrically cooled to -85^{o}C. Typical realized seeing is on the order of one arc-second, and the CCD is binned 4x4 resulting in approximately 2 pixels or 6 nm per seeing width. Typically, spectra are summed in 20 nm spectral bins, which will be sufficiently sampled even in poorer seeing conditions. This system did suffer from significant vignetting, requiring targets to be placed precisely at the same position on the chip. However, the setup was remarkably successful for the study of bright GEO targets (Dao, et al. 2013).

This prototype grating was also tested on some bright, well studied main belt asteroids. A typical image is shown in Figure 2 of the main belt asteroid 79 Eurynome taken under bright moon light conditions. The raw data product is a two-dimensional FITS image that contains both the zeroth- and first-order spectral image of the target. This frame has been bias- and dark current-subtracted using the IRAF *imred* package. However, since the current grating also introduces some vignetting, flat fields are acquired, and then the large scale gradients are removed before applying them to the object images. This has the effect of correcting for pixel-to-pixel variations while leaving the large scale gradients untouched, given that trying to separate these spatial gradients from color sensitivities is a dubious procedure at best. For slow moving, main belt asteroids, the zero-order image is placed near the edge of the unvignetted field which allows the full first-order spectra to be captured on the chip. When possible, we try to place any calibrations stars at the same position in an attempt to minimize effects of any large scale gradients ignored in the flat-fielding process. For the current work, ten images were taken and then realigned and summed.

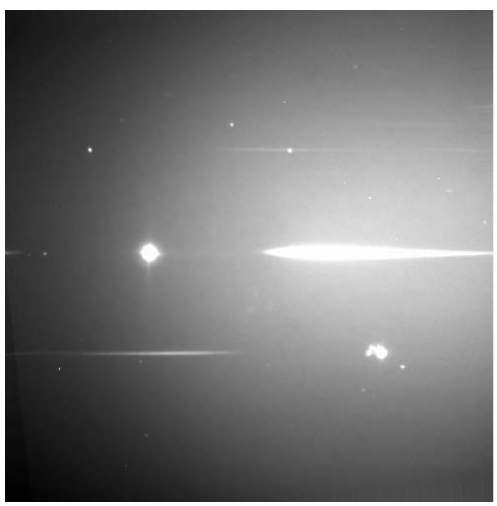

Fig. 2 Summed image consisting of ten 50 second exposures of asteroid 79 Eurynome which includes the zero- and first-order images captured horizontally along the center.

The standard procedure to extract a spectrum from the above image can be visualized in Figure 3. The signal within the enclosed strip depicted by the yellow lines is measured as a function of horizontal position. Similarly, a local background is determined as a function of horizontal position by averaging the two strips within the magenta lines. The background signal is normally determined using regions much larger than the one containing the signal. However, since the background is relatively smooth due to the bright moon light, the background regions are kept tight to ensure that the measured background is truly local for the heavily vignetted prototype system.

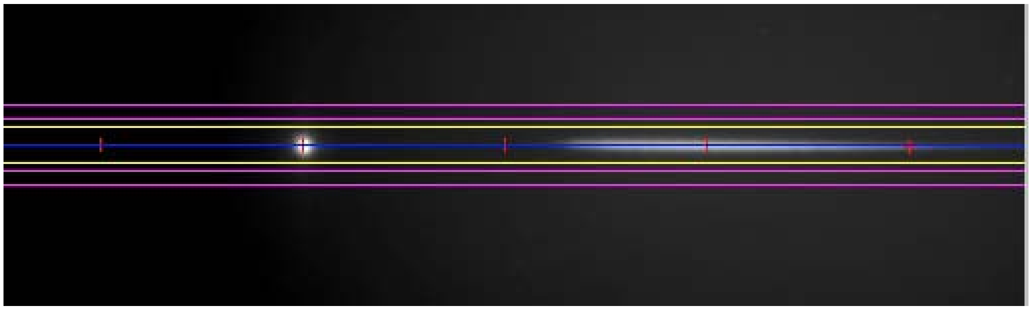

Fig. 3. Extraction fiducials for the grating spectrum of asteroid 79 Eurynome obtained using the MRO 2.4m telescope.

This overall extraction is accomplished making heavy use of the IDL *atv* procedure, resulting in the trace of the zeroth and first-order spectrum shown in Figure 4.

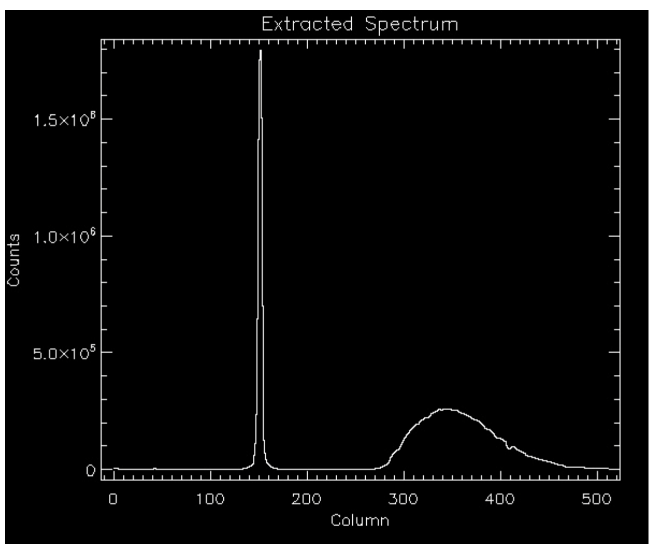

Fig. 4. Local background subtracted trace of the grating spectrum of asteroid 79 Eurynome.

Wavelength calibration is accomplished by performing the procedure on Wolf-Rayet stars with prominent emission lines of known wavelength to determine the dispersion per pixel. Then, using the zeroth order spectrum as the origin, the extracted spectrum can be calibrated as a function of wavelength as depicted in Figure 5. This and the subsequent analysis was accomplished using custom IDL software routines.

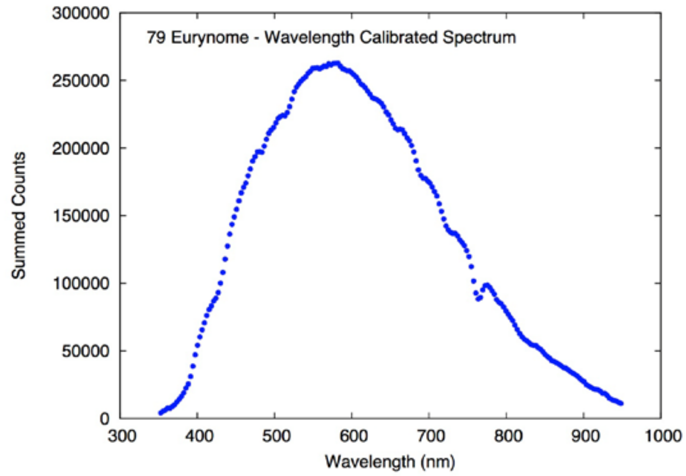

Fig. 5. Wavelength-calibrated spectrum of 79 Eurynome taken with the 2.4-meter telescope in August, 2012.

At this point, the next step would typically be to calibrate the instrumental counts to flux units using known photometric standards. However, for taxonomic classifications of asteroid spectra, surface reflectance is the primary quantity of interest. Therefore, the process needed is to correct for the Sun's illuminations of the target. To accomplish this, spectra are taken of known solar analogs under identical (or corrected to identical) observing conditions and instrumental setup. Determining the reflectance is then a matter of dividing the observed target spectra by that of a solar analog. Figure 6 shows the results of this procedure for the S-type asteroid 79 Eurynome and C-type asteroid 59 Elpis using the well known solar analog Hyades 64.

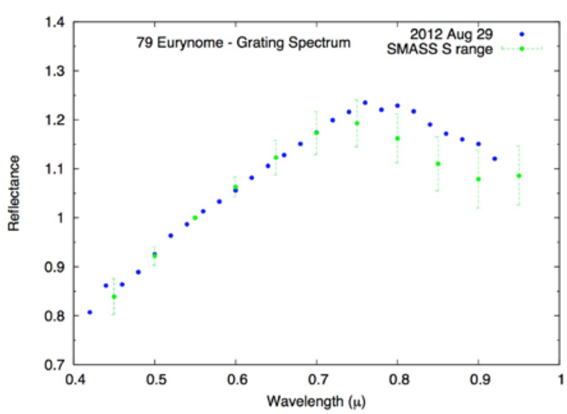

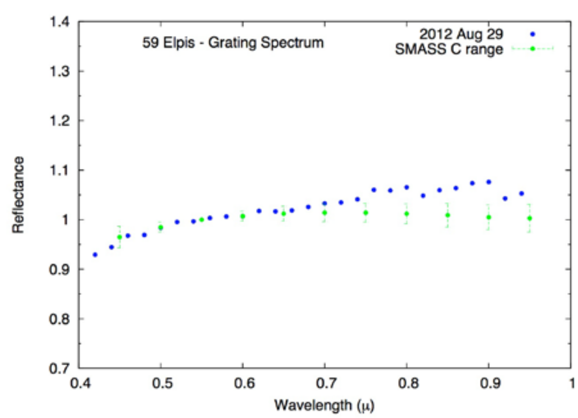

Fig. 6. Reflectance spectra of 79 Eurynome (left) and 59 Elpis (right) obtained using the MRO 2.4-meter telescope in August, 2012.

Overplotted in each case are the average ranges of typical S- and C-class spectra from the SMASS catalog. In both cases, there is a slightly enhanced signal at the red end. This is likely error introduced from poor background subtraction while testing highly vignetted prototype in bright moon light. However, this test indicated that for bright (~10-11) targets a least, S- and C-type asteroids can be reliably distinguished using this simple, rapidly deployable system.

Upgraded Slitless Grating Configuration

A larger 75 lines/mm grating, resulting in a dispersion of 75 nm/mm and minimal vignetting, has since been acquired. An image displaying a typical bright target spectra with a relatively flat, unvignetted background is shown in the 6 second exposure of the solar analog SA 102-1081 in Figure 7.

Fig. 7. Zeroth and first order images of solar analog SA 102-1081 displaying the minimal vignetting when using the larger grating.

On March 6, 2014, the recently discovered near-Earth asteroid 2014 EC made a close approach to Earth, providing an opportunity to test the grating spectra technique for a real target of opportunity with scientific interest. A single 60 second exposure of this object is shown in Figure 8. As can be seen, the spectral signature is rather low. However, exposure times were limited by the buildup of the fringing pattern due to the interference of the sky emission lines and the small surface variations of the back illuminated CCD.

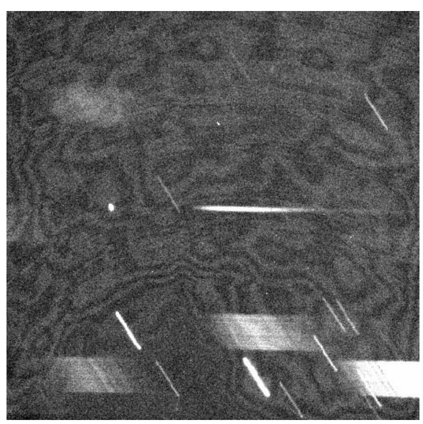

Fig. 8. A single 60 second exposure of the visible magnitude V~17 near-Earth asteroid 2014 EC is shown. The field stars can be seen as moving diagonally while the telescope is tracking on the asteroid moving at ~30 arc-second per minute.

The primary motivation driving the need for an unvignetted slitless grating system was to remove the requirement of precise positioning of the target and calibration star at the same location on the chip, allowing for easier acquisition of the spectra of fast moving artificial targets. However, this also allows us to dither images of targets that require longer exposures to varying places in the fringe pattern. Therefore to obtain a measurable spectrum of 2014 EC, 10 images were acquired and added together with the target shifted in each image, averaging out the two dimensional background. The spectrum is then extracted and averaged in the manner described above, and the results are shown in Figure 9.

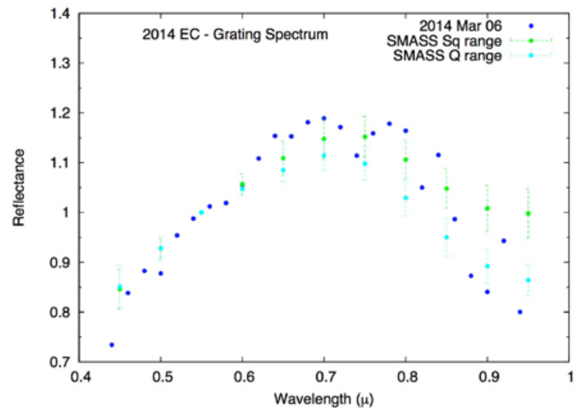

Fig 9. Spectrum of the NEO 2014 EC acquired using the simple grating system in the filter wheel of the MRO 2.4-meter telescope.

This can be contrasted to the spectrum acquired using the slit-based MOSS instument on the same night which is shown in Figure 10.

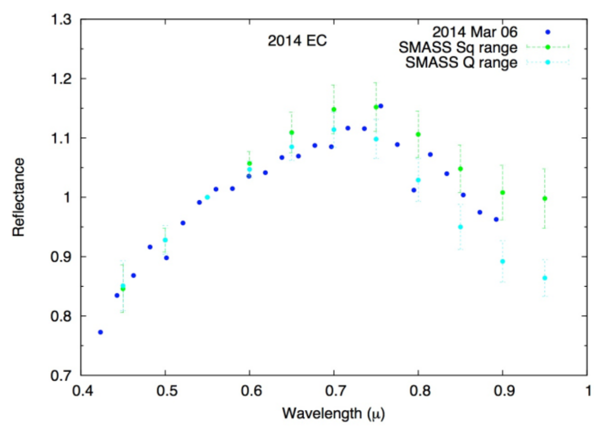

Fig. 10. Visible spectra (right) of 2014 EC (dark blue symbols) obtained using MOSS on March 6, 2014 indicates a Sq-Q-type composition (silicate/metallic). The mean SMASS Q and Sq values (green/light blue symbols) are overplotted to illustrate how the compositional determination is estimated.

3. CONCLUSIONS

It is clear from Figures 9 and 10 that the MOSS spectrometer provides a less noisy spectrum than the simple slitless grating system under similar conditions. However, Figure 9 shows that the Sq/Q nature of 2014 EC was still easily discernible using the simple grating mounted in the 2.4-meter telescope facility filter wheel. This implies that this system has the potential to obtain rough taxonomic classifications of target of opportunity objects as faint as visible magnitude V~17 when the MOSS spectrometer is unavailable. Future work will involve determining how faint an asteroid can be characterized for material composition employing this simple grating technique.

4. ACKNOWLEDGEMENTS

This research is funded through NASA's Near-Earth Objects Observations (NEOO) program.

We also thank Lee Johnson (JPL) for his assistance in acquiring the MOSS-based comparison spectra shown in Figure 10.

7. REFERENCES

1. Dao, P., P. McNicholl, A. Dentamaro, E. Ryan, and William Ryan (2013). Unmixing Space Object's Moderate Resolution Spectra. *2013 AMOS Technical Conference*, Maui, Hawaii.

2. Binzel, R.P., Lupishko, D., Di Martino, M., Whiteley, R.J., and Hahn, G.H., Physical Properties of Near Earth Objects, In *Asteroids III*, (Bottke, W.F., Cellino, A., Paolicchi, P., and Binzel, R. P., Eds., University of Arizona Press, Tucson) 255-272, 2002.

3. Binzel, R. P., Rivkin, A. S., Stuart, J. S., Harris, A. W., Bus, S. J., and Burbine, T. H., "Observed spectral properties of near-Earth objects: results for population distribution, source regions, and space weathering processes", *Icarus* **170**, 259-294, 2004.

4. Stuart, J. S., and Binzel, R. P., Bias-corrected population, size distribution, and impact hazard for the near-Earth objects, *Icarus*, **170**, 295-311, 2004.